Anal. Chem. **XXXX,** *xxx,* 000–000

Combined X-ray Diffraction and Raman Identification of Synthetic Organic Pigments in Works of Art: From Powder Samples to Artists' Paints

L. B. Brostoff,*,†,∥ S. A. Centeno,*,‡ P. Ropret,§,∥ P. Bythrow,∥ and F. Pottier∥

Preservation Research and Testing Division, Preservation Directorate, The Library of Congress, 101 Independence Avenue SE, Washington, D.C. 20540, The Metropolitan Museum of Art, 1000 Fifth Avenue, New York, New York 10028, Institute for the Protection of the Cultural Heritage of Slovenia, Restoration Center, Poljanska 40, 1000 Ljubljana, Slovenia, and Museum Conservation Institute, Smithsonian Institution, 4210 Silver Hill Road, Suitland, Maryland 20746

X-ray diffraction (XRD) complemented by Raman spectroscopy analyses of synthetic organic pigments in powder samples, layered paint systems, and commercial artists' paints bound in acrylic, alkyd, and oil media are presented. The potential and limitations of the techniques to identify and characterize mixtures of these pigments, along with inorganic extenders, in works of art are exemplified and discussed. Stratified model paint systems that mimic the layering structure typically found in modern paintings are used to evaluate the effect of the μXRD experimental parameters, as well as extenders or fillers commonly found in modern artists' paint formulations, on the quality of the patterns recorded in microsamples of paint. XRD is demonstrated for the first time to be an effective tool for the specific identification of synthetic organic pigment mixtures and fillers in acrylic and alkyd bound artists' paints, while the identification of these pigments by XRD in oil bound paints appears problematic. Detailed crystallographic information provided by XRD is shown to be complementary to molecular information provided by Raman analysis. The combined use of these techniques allows for more frequent unambiguous compound identification than would be possible using one technique alone.

The identity of artists' pigments has important bearing on both the history and the conservation of works of art. Pigment identity is often a key element in understanding artists' techniques, especially for purposes of dating, attribution, and detection of forgeries (see, for example, refs 1–3). The identification and characterization of pigments and binding media in artists' materials are also crucial for designing safe conservation treatments, as well as for determining suitable environmental conditions for display, storage, and transport of works of art.

Modern and contemporary paints and other media are rife with modern synthetic organic pigments (SOPs). Development of these types of pigments began in the second half of the 19th century after Perkins first synthesized mauve in 1856[4–6] and has continued through the present day. Besides SOPs, modern paint formulations include a variety of synthetic binding media, such as acrylic, alkyd, polyvinyl acetate, and nitrocellulose, plus numerous types of surfactants, thickeners, defoamers, pH buffers, and other additives. Both the pigments and the binding media in modern and contemporary paint formulations significantly affect the aging behavior and stability of the paint layers under a wide variety of conditions, including light, temperature, and relative humidity.[7–9] In addition, modern artists tend to mix materials that are not intended for artists' use into their formulations, including, for example, paint developed for other applications.[9] Therefore, the conservation of these complex modern artists' paints generally requires different approaches than those developed for traditional painting materials.

Some of the standard techniques used to analyze paints in works of art for their technical study and conservation, including various types of microscopy, energy dispersive X-ray spectroscopy (EDS), X-ray fluorescence (XRF), and Fourier transform infrared spectroscopy (FT-IR), offer limited utility when applied to the

* To whom correspondence should be addressed. E-mail: lbrostoff@loc.gov (L.B.); silvia.centeno@metmuseum.org (S.A.C.).

† The Library of Congress.

‡ The Metropolitan Museum of Art.

§ Institute for the Protection of the Cultural Heritage of Slovenia.

∥ Formerly at the Smithsonian Institution.

(1) Cooper, H.; Khandekar, N.; Mancusi-Ungaro, C.; Rosenberger, C.; Eremin, K.; Kirby, D.; Smith, K.; Stenger, J. *Technical Analysis of Three Paintings Attributed to Jackson Pollock*; Harvard University Art Museums: Cambridge, MA, Jan. 31, 2007; http://www.artmuseums.harvard.edu/home/HUAMreport012907.pdf.

(2) Centeno, S. A.; Mahon, D.; Wypyski, M. T. *J. Raman Spectrosc.* **2004**, *35*, 774–780.

(3) Edelstein, B.; Centeno, S. A.; Wypyski, M. T. In *The Object in Context: Crossing Conservation Boundaries*; Saunders, D., Townsend, J. H., Woodcock, S., Eds.; International Institute for Conservation of Historic and Artistic Works: London, 2006; pp 204–210.

(4) Zollinger, H. *Color Chemistry. Syntheses, Properties, and Applications of Organic Dyes and Pigments.* Wiley-VCH: Zürich, 2003.

(5) Herbst, W.; Hunger, K. *Industrial Organic Pigments*, 3rd ed.; Wiley-VCH: Weinheim, Germany and New York, 2004.

(6) Colour Index International, 4th ed. Online. The Society of Dyers and Colourists and the American Association of Textile Chemists and Colorists; http://www.colour-index.org, (January 2009).

(7) Learner, T. J. S.; Chiantore, O.; Scalarone, D. In *Preprints of the 13th Triennial Meeting of the ICOM Committee for Conservation*; James and James: London, 2002; p 911.

(8) Learner, T. J. S. *Analysis of Modern Paints*; The Getty Conservation Institute: Los Angeles, CA, 2004.

(9) Learner, T. J. S. *Proc. Natl. Acad. Sci. U.S.A.* **2005**, 137.

10.1021/ac9004953 CCC: $40.75 © XXXX American Chemical Society

analysis of SOPs. This is due primarily to the general lack of metals in their composition and/or the dominance of the binding medium in the detection of organic phases. More recently, Raman spectroscopy has been demonstrated to offer a significant advance in the study and identification of SOPs, particularly as a noninvasive technique.[10−13] However, for the identification of a number of these pigments, Raman spectroscopy has limitations, due to fluorescence and interference from extenders and other components in the paint formulation.[11−13]

In the paint industry, X-ray diffraction (XRD) is routinely used for the characterization of SOP powder samples.[14−17] The technique has also been used to examine inorganic pigments in paint samples,[14] but to our knowledge the use of XRD has not been reported for the study of SOPs in the presence of a binding medium. In the conservation field, while XRD has been widely used for the analysis of inorganic pigments and deterioration products either in microsamples from artworks or in situ (see for example refs 18−21), it has been generally overlooked as a method for the identification and study of SOPs in modern works of art.

Many important artists' pigments, especially the polycyclic pigments, including copper phthalocyanine blue, quinacridone, indanthrone, dioxazine, and some azo pigments, exist in different polymorphic forms that may be pure, mixed crystals, or solid solutions. The crystal form of a pigment is a key determinant in such physical properties as hue, density, hardness, melting point, particle size, and shape. Important application properties of SOPs that affect both the durability and conservation of artist's paints can vary considerably with crystallinity. Such properties include tinctorial strength, hiding power, rheology, heat and solvent resistance, and light and migration fastness. Generally, properties of a pigment such as lightfastness and the ability to disperse improve with larger and more perfect crystals, although dispersion is also driven by chemical affinity with the binding medium. Slight variations in manufacturing processes, including pH, drying procedure, drying temperature, and the milling method, may cause the transformation of polymorphs, as well as affect the degree of crystallinity and crystal quality. The manufacture of SOPs usually results in the formation of relatively large-sized crystals with significant impurities. Therefore, the product requires some form of particle size reduction in the range of 0.10−10.0 μm and/or purification to be useful as a pigment in inks and paints.[5,15,17,22]

In this particle range, XRD is ideal for revealing a unique diffraction pattern, or an additive phase pattern, that contains the fingerprints of individual pigments and extenders in paint mixtures. Crystallites smaller than about 500 nm, as well as crystal strain and imperfections, tend to broaden the diffraction peaks in a spectrum, while larger, more perfect crystallites produce sharper peaks. Shifts in the *d*-spacings or changes in the relative intensities of peaks normally indicate a transition from one crystal phase to another or a change in the composition of a solid solution; loss of peaks or the creation of new ones may indicate subtle conversion to a new crystalline phase.[4,22] XRD thus has the potential of establishing the chemical identity of crystalline SOPs and fillers, as well as distinguishing a pigment's polymorphism and crystal quality. XRD is also an unexplored tool for the study of changes in SOP crystallinity and particle size that may result from aging, environmental conditions, or conservation treatments.

This article presents a novel application of XRD as both a standalone and complementary technique to Raman spectroscopy for the analysis of SOPs (a) as pure powders, (b) in model stratified paint samples, and (c) in actual commercial artists' paints with three major types of binders: acrylic, alkyd, and oil. The study demonstrates the utility and potential of XRD to identify and study these types of pigments in paint films, especially in combination with Raman analysis, as well as to indicate crystal form and purity, which may have significant bearing on heat and lightfastness, purity, and solubility. This new analytical approach to the study of works of art also allows a more complete characterization of specific commercial paint products that contain SOPs and other associated compounds, which is often quite helpful, for example, in the detection of forgeries.

EXPERIMENTAL SECTION

Measurements were carried out on three different sample groups: commercial SOP powders, stratified model paint systems, and commercial paint samples containing SOPs, with or without inorganic fillers, bound in acrylic, alkyd, and oil binders, respectively. All commercial pigment powder samples (Table 1) were analyzed as received from the manufacturer without further preparation or grinding in order to avoid possible polymorphic phase changes.[22] Pigments are referred to by their color index (CI) generic names. CI names are composed of the letter P, a letter that describes the hue (R stands for red, Y for yellow, etc.), and a number. These commercial pigment powder samples were generously provided by SunChemicals, Clariant, Ferrario, Ostacolor, Schmincke, Kremer, Maimeri, and Ciba. XRD patterns of the commercial powder samples were used as references along with powder diffraction files (PDFs) contained in the International Center for Diffraction Data (ICDD) pigment database.

To estimate the penetration depth of the X-rays in a paint flake with respect to sample and beam geometry, layered model paint samples consisting of a top layer of a pure SOP (PR 146, PY 1, PY 73, PY 74, or PY 83), a middle layer of TiO_2 (rutile), and a bottom layer of $CaCO_3$ (calcite) were constructed. Each layer of pigment or filler material was hand mixed with Liquitex acrylic gel medium, which is amorphous and thus does not produce XRD peaks. Construction of the model paint samples was carried out by first setting the middle layer of TiO_2 on a sheet of Mylar and then drawing out the remaining two components onto either side after appropriate drying. The

(10) Vandenabeele, P.; Moens, L.; Edwards, H. G. M.; Dams, R. *J. Raman Spectrosc.* **2000**, *31*, 509–517.
(11) Centeno, S. A.; Lladó Buisan, V.; Ropret, P. *J. Raman Spectrosc.* **2006**, *37*, 1111–1118.
(12) Ropret, P.; Centeno, S. A.; Bukovec, P. *Spectrochim. Acta, Part A* **2008**, *69*, 486–497.
(13) Schulte, F.; Brzezinka, K.-W.; Lutzenberger, K.; Stege, H.; Panne, U. *J. Raman Spectrosc.* **2008**, *39*, 1455–1463.
(14) Scott, R. W. *J. Paint Technol.* **1969**, *41*, 422–430.
(15) Hao, Z.; Iqbal, A. *Chem. Soc. Rev.* **1997**, *26*, 203–213.
(16) Kamarchik, P.; Cunningham, G. P. *Prog. Org. Coat.* **1980**, *8*, 81–107.
(17) Debnath, N. C.; Vaidya, S. A. *Prog. Org. Coat.* **2006**, *56*, 159–168.
(18) Chiari, G.; Giordano, A.; Menges, G. *Sci. Technol. Cultural Heritage* **1996**, *5* (1), 21–36.
(19) Van Loon, A.; Boon, J. J. *Spectrochim. Acta, Part B* **2004**, *59*, 1601–1609.
(20) Correia, A. M.; Oliveira, M. J. V.; Clark, R. J. H.; Ribeiro, M. I.; Duarte, M. L. *Anal. Chem.* **2008**, *80*, 1482–1492.
(21) Chiari, G.; Sarrazin, P. (Oral and poster presentation), Denver X-ray Conference, Denver, CO, 2008.
(22) Whitaker, A. *JSDC* **1986**, *102*, 66–76.

Table 1. Pigment Powder Samples Analyzed by μXRD (Cu Kα radiation)

color index name	manufacturer/name	alternative commercial names	pigment class[a]/chemical formula[b]	ICDD powder diffraction file (PDF #) match
PY 1	SunChemicals/ Sunbrite Yellow 1	Hansa Yellow G	Monoazo Yellow/$C_{17}H_{16}N_4O_4$	PY 1 (32-1720, 36-1854); Barite (24-1035)
PY 3	SunChemicals/ Sunbrite Yellow 3	Hansa Yellow Light	Monoazo Yellow/$C_{16}H_{12}Cl_2N_4O_4$	PY 3 (36-1855); Rutile (21-1276); Barite (24-1035)
PY 65	SunChemicals/ Sunbrite Yellow 65		Monoazo Yellow/$C_{18}H_{18}N_4O_6$	PY 65 (38-1553); Barite (24-1035)
PY 74	SunChemicals/ Sunbrite Yellow 74	Hansa Yellow I; Hansa Yellow Med.	Monoazo Yellow/$C_{18}H_{18}N_4O_6$	PY 74 (36-1862); Barite (54-1035)
PY 83	SunChemicals/ Sunbrite Yellow 83	Diarylide Yellow I; Indian Yellow	Diarylide Yellow/$C_{36}H_{32}Cl_4N_6O_8$	PY 83 (47-2129); (?) γ-Diazo pigment (43-1647)
PY 97	Clariant/Novoperm Yellow FGL		Monoazo Yellow/$C_{26}H_{27}ClN_4O_8S$	PY 97 (47-2130); (?) Kaolinite (14-0164)
PR 5	Ferrario/PR 5		Naphthol AS/ $C_{30}H_{31}ClN_4O_7S$	PR 5 (36-1805)
PR 9	Kremer/ Permanentrot FRLL	Naphthol Red II; Naphthol Scarlet	Naphthol AS/$C_{240}H_{17}Cl_2N_3O_3$	PR 9 (47-2124)
PR 83	Schmincke/Alizarin Madder Deep	Alizarin crimson	(1,2-dihydroxy-anthraquinone, Al, Ca)[a]	No matches found
PR 122	Clariant/Hostaperm Pink E-TS	Quinacridone Magenta	Quinacridone/$C_{22}H_{16}N_2O_2$	PR 122 (36-1799)
PR 146	EcPigments/Eljon Carmine LBB 56128F	Naphthol Red III	Naphthol AS/$C_{33}H_{27}ClN_4O_6$	PR 146 (36-1795)
PR 170	Clariant/Novoperm Red F2RK 70		Naphthol AS/$C_{26}H_{22}N_4O_4$	PR 170 (36-1793)
PR 264	Ciba/Irgazin DPP rubine FTX		($C_{30}H_{20}N_2O_2$)[a]	no matches found
PV 19	Ciba/Cinquasia Violet R NRT-201-D	β-Quinacridone Violet I; Quinacridone Red or Violet	Diketopyrrolo-pyrrole (DPP)/$C_{20}H_{12}N_2O_2$	PV 19 (36-1850)
PV 23	SunChemicals/ Sunfast Violet 23	Dioxazine Purple	Dioxazine/$C_{34}H_{22}Cl_2N_4O_2$	PV 23 (47-2132)
PG 7	Clariant/Hostaperm Green GNX	Phthalo Green	Cu-Phthalogreen/$C_{32}H_{16-x}Cl_xCuN_8$	PG 7 (36-1870)
PG 8	Maimeri/PG 8	Hooker's Green NL	Metal complex/$C_{30}H_{18}FeN_3NaO_6$	PG 8 (36-1873); Barite (24-1035)
PO 34	Clariant/Permanent Orange RL 70		Disazopyrazolone/$C_{34}H_{26}Cl_2N_8O_2$	PO 34 (47-2158)
PB 15:3	Ostacolor/Versal Blue LBS	β-Copper Phthalocyanine	Cu-Phthaloblue, β mod/$C_{32}H_{16}CuN_8$	β-Copper Phthalocyanine (11-0893); PB 15:4 (36-1881)

[a] See ref 5. [b] ICDD PDF database, if not otherwise marked; ? = tentative phase identification.

resulting samples mimicked the overall thickness of the commercial paint samples described below, as well as the stratification of a generic sample from a work of art.

The commercial paint samples chosen for analysis, along with their compositions as declared by the manufacturers, are as follows: Gruden (Professional) Permanent Red Deep (PR 146) acrylic, Gruden (Professional) Yellow Medium Azo (PY 1) acrylic, Ferrario (Maxcrill) Giallo Hansa Medio (PY 83) acrylic, Ferrario (Alkyd) Lacca Garanza Rosa (PV 19, PR 83) alkyd, Lukas (Studio) Echtrot (PO 34, PR 9) oil, Lukas (Studio) Brillantgelb hell (PY 1, ZnO, lithopone) oil, Lukas (Studio) Primaire-blau (PB 15:3, ZnO) oil, Ferrario (IdrOil) Verde Vescica (PG 8, PY 83) oil, and Lefranc and Bourgeois (Louvre) Sap Green (PG 8) oil (Table S-1 in the Supporting Information). These samples were drawn out onto glass slides and air-dried.

Micro-X-ray diffraction (μXRD) measurements were carried out at the Smithsonian Institution's Museum Conservation Institute (MCI) on a Rigaku D/Max Rapid X-Ray microdiffractometer outfitted with a graphite plate crystal monochromator and an imaging plate detector, which allows integration of the diffraction rings so that preferred orientation effects are minimized. The instrument was operated using Cu Kα ($\lambda = 1.542$ Å) radiation at 200 kW (50 kV acceleration voltage and 40 mA current) and, for a subset of paint film samples, using Cr Kα radiation ($\lambda = 2.291$ Å) at 179 kW (46 kV acceleration voltage and 39 mA current). SOP powders and commercial paint film samples were mounted on the end of glass fibers in a collimated beam with goniometer parameters as follows: χ fixed at 45°, ω fixed at 1, 2, or 3°, and φ spun through 360° rotation at 1°/s. The X-ray beam was collimated for most Cu Kα exposures to 0.3 mm and exposed for 15 min; in select cases, samples were exposed for 2−4 h using a 0.1 mm collimator. The X-ray beam was collimated for Cr Kα exposures to 0.3 or 0.8 mm and exposed for 2 h or 30 min, respectively. The model paint samples were mounted perpendicularly on the end of glass fibers and examined under similar conditions, but at varying ω angles of incidence in order to gauge the depth of penetration of the X-ray beam, as discussed below.

Select X-ray diffraction measurements were also carried out in a Philips PW1835 open architecture design, Bragg−Brentano focusing system diffractometer using Cu Kα radiation (45 kV acceleration voltage and 35 mA current). Commercial pigment powder samples were mounted on scotch tape and adhered to glass microscopy slides. Commercial artists' paints were analyzed in situ as applied to microscopy glass slides using a 10 × 2 mm mask. In addition to the sample holder, the instrument includes an approximately 15 cm wide and 17 cm deep platform that allows the in situ examination of relatively small art objects.

Raman spectroscopy measurements were carried out with a Renishaw System 1000 coupled to a Leica DM LM microscope. The pigment powders and commercial paint samples as applied to glass microscopy slides were first examined using polarized light and UV illumination in the microscope attached to the spectrometer to establish that not more than one phase existed. Raman spectra were then recorded by focusing a 785 nm laser

beam using a 50× objective lens. Neutral density filters were used to set the laser power at the sample to values between 0.2 and 1.5 mW. A 1200 lines/mm grating and a thermoelectrically cooled CCD detector were used, with integration times between 10 and 60 s.

RESULTS AND DISCUSSION

Synthetic Organic Pigment Powders. The μXRD patterns of 19 synthetic organic pigment (SOP) powder samples were measured using Cu Kα radiation. Experimental diffraction patterns were matched with reference powder diffraction patterns (PDFs) in the ICDD database using Jade 7.0 software; this allowed unambiguous phase identification in the majority of the cases, as shown in Table 1, although many of the experimental diffraction patterns contain one or more unidentified peaks (see Tables S-2–S-20 in the Supporting Information). As has been noted by other authors,[15–17] unidentified peaks in diffraction patterns for SOPs may arise from impurities, while mixed crystals may cause a unique diffraction pattern, which complicates identification by XRD. It is also worth noting that the ICDD database is not perfect and, particularly in older experimental data, there commonly are missing peaks and incorrect intensities. Individual cases relevant to the stratified paint samples and the commercial paints analyzed in the present study are further discussed below.

An example of a typical μXRD diffraction pattern obtained from a pure SOP powder sample is that of PY 1 (SunChemicals), a monoazo yellow pigment (Figure 1A, Table S-2 in the Supporting Information). Here, the raw pattern (top) is shown together with the pattern after subtraction of the amorphous background (bottom), the main component of which is attributed to the glass fiber mount. Searching in the ICDD database in this case produced very good pattern matching for barite ($BaSO_4$), a common pigment extender, and two PY 1 reference patterns. These phases account for nearly 100% of the peaks in the experimental pattern. While the two PY 1 reference patterns are in good agreement with each other, allowing for minor shifting, only the pattern supplied by A. Whitaker (PDF #32-1720) is indexed (revealing a monoclinic crystal cell structure) and, therefore, has a higher quality rating; this pattern also exhibits more lines and generally stronger peak intensities. The experimental SOP pattern is in excellent agreement with Whitaker's pattern, showing *d*-spacing shifts in only the range of 0.00–0.02 Å and relatively sharp and well-defined peaks (Table S-2 in the Supporting Information). Since it is known that PY 1 has only one crystal form,[23] the experimental SOP pattern thus indicates that this powder specimen is a well-crystallized sample of high quality.

Figure 1B shows the experimental diffraction pattern, with and without background subtraction, obtained by μXRD for the pure powder sample PV 19 (Ciba), an unsubstituted quinacridone pigment. The quinacridones are polycyclic organic compounds, the linear trans forms of which have found industrial importance as pigments since the end of the 1950s. PV 19 is known to have at least three major crystal structures, the β and γ crystal forms of which are the most stable and important from a commercial point of view;[23,24] the δ and ε forms, as well as variants of the γ form, have also been identified[24–26] but are not widely accepted.[25,26] It has been hypothesized that deviant X-ray powder diffraction results arise primarily from variations in the crystallite size and shape of specimens.[23,27,28] The polymorphism of this pigment is known to strongly affect hue and lightfastness and has been comparatively well-studied.[5,22–28]

The experimental diffraction data obtained from the PV 19 powder sample is shown in Table 2 (and Table S-15 in the Supporting Information) along with selected reference pattern data. It is noted that the PDF designated as PV 19 in the ICDD database is not identified by crystal form, nor is it indexed, and therefore has a quality mark of doubtful. Agreement between experimental and published diffraction data is shown to be excellent in terms of *d*-spacing, while agreement in terms of relative peak intensity is best with the ICDD reference. The experimental pattern also exhibits several unidentified peaks, including those near 12.33 and 6.62 Å, which appear quite broad in contrast to the identified quinacridone peaks. This suggests the existence of a secondary phase with small and/or strained particles. In addition, the relatively sharp and prominent unidentified peak near $d = 4.11$ Å suggests the existence of either an impurity or an additional quinacridone polymorph. These results indicate that the laboratory powder sample may be characterized as a multiphase material consisting predominantly of the β-quinacridone form of PV 19 pigment.

The experimental XRD patterns discussed above are typical of those obtained from the 19 pure pigment powders examined in this study. Results may be generalized as follows. Minor shifts in the *d*-spacings and intensity ratios may often be observed in experimental patterns compared to reference PDFs found in the ICDD database (see Tables S-2–S-20 in the Supporting Information). These *d*-spacing shifts, which can be fairly large at small 2θ angles, may be due to the fact that patterns in the ICDD database are normally generated from analytically pure crystalline materials, or single crystals, rather than industrial-grade samples. However, as mentioned above, line shifts and relative intensity differences may indicate mixed crystals or subtle crystal modifications, which can be caused by even slight variations in the manufacturing process.[5,26] Similar shifts in XRD patterns obtained from laboratory samples have been previously reported by other authors,[17,22] including line broadening and relative intensity changes from variations in crystallite size and/or strain, along with additional diffraction lines from impurities.[23] While small contributions to both line shifting and broadening from instrumental parameters, including sample mounting and alignment methods, cannot be discounted, results clearly point out that individual samples of SOPs and polymorphic SOPs, in particular, as used in artists' paints, may be poorly understood in terms of their crystallographic variations and quality. In addition, these experimental patterns stand themselves as new XRD references for specific commercial artists' pigments that will allow their future recognition in works of art.

(23) Whitaker, A. In *The Analytical Chemistry of Synthetic Dyes*, Venkataraman, K., Ed.; John Wiley & Sons, Inc.: Canada, 1977, pp269–298.

(24) Filho, D. S.; Oliveira, C. M. F. *J. Mater. Sci.* **1992**, *27*, 5101–5107.

(25) Potts, G. D.; Jones, W.; Bullock, J. F.; Andrews, J.; Maginn, S. J. *Chem. Soc. Chem. Commun.* **1994**, 2565–2566.

(26) Lincke, G. *J. Mater. Sci.* **1997**, *32*, 6447–6451.

(27) Whitaker, A. *JSDC* **1977**, (Jan.), 15–17.

(28) Panina, N.; Leusen, J. J. J.; Janssen, F. F. B. J.; Verwer, P.; Meekes, H.; Vlieg, E.; Deroover, G. J. *Appl. Cryst.* **2007**, *40*, 105–114.

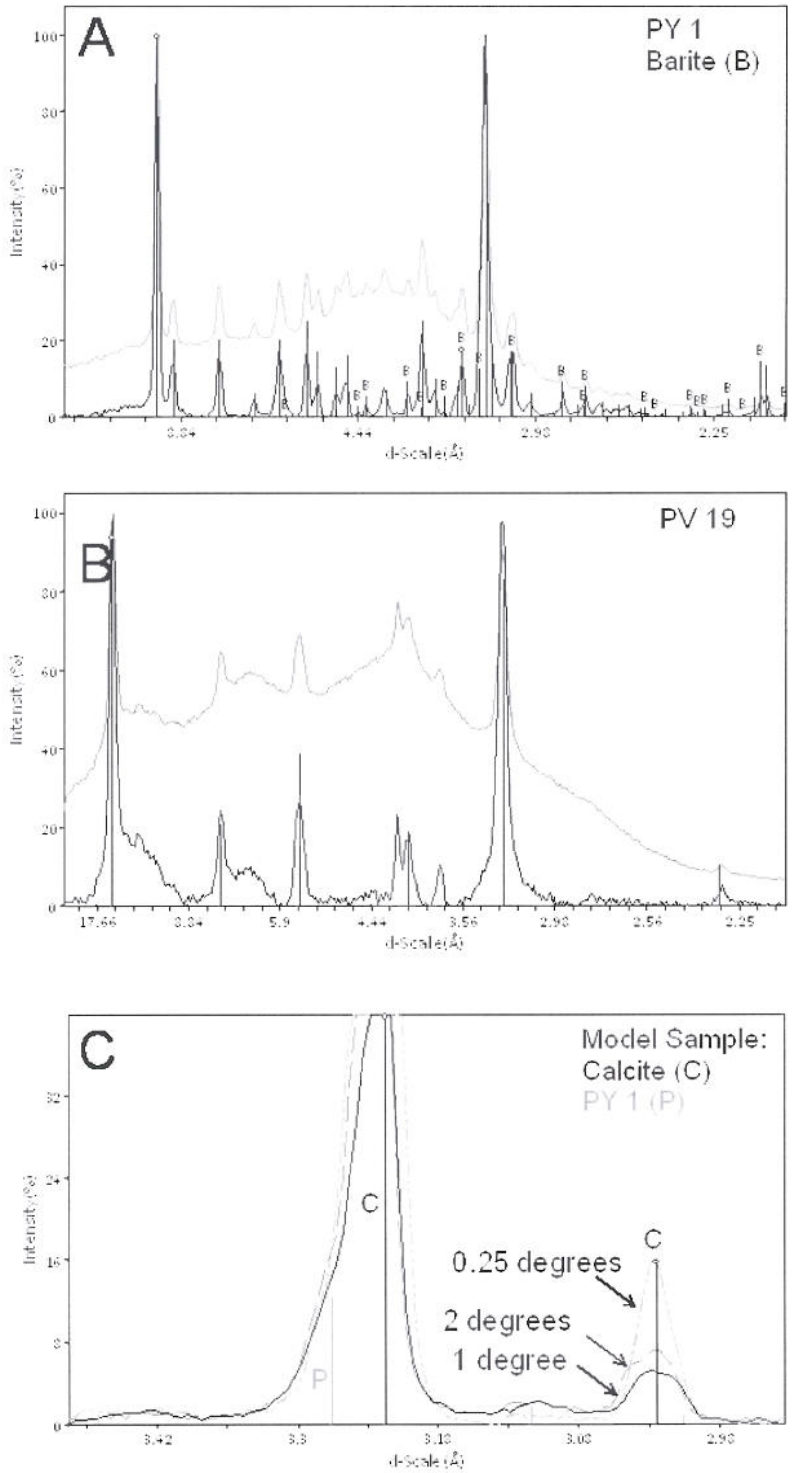

Figure 1. μXRD patterns (Cu Kα radiation) of pure pigment powder samples and ICDD pattern matches (vertical bars) of: (A) PY 1 (SunChemical), raw pattern (above) and background subtracted (below; barite marked with "B"); (B) PV 19 (Ciba), raw pattern (above) and background subtracted (below); and (C) model PY 1 (SunChemicals) system taken at various ω angles, normalized to PY 1, showing comparison of 100% line of calcite.

Model Paint Systems. In order to better understand the role of beam geometry, paint additives, and layering structure in the XRD analysis of a stratified paint flake, model paint systems were constructed and examined by μXRD at various angles of incidence with respect to the sample surface. As mentioned above, the model samples consisted of a top layer of SOP, a middle layer of TiO_2 (rutile), and a bottom layer of $CaCO_3$ (calcite); each layer of pigment or filler material was mixed with an acrylic binder. The thickness of the top paint layer containing the SOP was typically on the order of 45 μm; the TiO_2 layer was about 30 μm, and the calcite layer was approximately 45 μm. The resulting samples mimicked the layering structure generally

Published on July 6, 2009 on http://pubs.acs.org | doi: 10.1021/ac9004953

Table 2. XRD Peak Table for Paint Sample 1AD (Ferrario (Alkyd) Lacca Garanza Rosa) and Pure Pigment Reference Powders PV 19 (Ciba) and PR 83[a]

	1AD (fresh film)		1AD		1AD		PR 83 (Schmincke)		PV 19 (Ciba) unknown modification		β-quinacridone		α-quinacridone		γ-quinacridone	
	μXRD (Cr Kα)		μXRD (Cu Kα)		open architecture XRD (Cu Kα)		μXRD (Cu Kα)		μXRD (Cu Kα)		PDF #41-1870 (Co Kα)		PDF #48-2090 (Cu Kα)		PDF #25-1782 (Cu Kα)	
phase identification	*d* (Å)	*I* (%)	*d* (Å)	*I* (%)	*d* (Å)	*I* (%)	*d* (Å)	*I* (%)	*d* (Å)	*I* (%)	*d* (Å)	*I* (%)	*d* (Å)	*I* (%)	*d* (Å)	*I* (%)
PV 19, β mod					15.1 (sh)	100			15.1	100	14.7	45				
PV 19, α mod	14.1	100	14.1	100	14.1−14.2	100							14.2	100		
PV 19, γ mod	shoulder	100	13.6	100	13.5−13.8	100									13.6	100
									12.3	15						
PR 83	11.2 (b)	100	11.5	100	11.5 (b)	100	11.3	100								
PR 83	9.96 (b)	57					9.98	24								
PR 83	8.38 (b)	31					8.53	19								
PV19, β mod (+gypsum?)			7.59		7.68 (s)				7.51	23	7.51	30				
PR 83/PV19, α mod	7.05	34					7.14	40					7.13	28		
PV 19, γ mod (+ unidentified phase?)	6.76	34	6.76	25											6.75	25
PR 83/PV 19, γ mod	shoulder		shoulder				6.64	9	6.62	8					6.58	20
PV 19, α and γ mod	6.42 (b)	81	6.40 (b)	40	6.39/6.44 (b)						6.38	7	6.32	62	6.39	40
	6.13	25														
PR 83	5.75	37					5.76	17								
PV 19, β mod									5.51	27	5.52	40				
PV 19, α mod	5.31	20			5.34								5.33	5		
					5.08											
PV 19, β mod (+ unidentified phase?)					4.86/4.89						4.92	3				
			4.77		4.76											
PV 19, α mod							4.48	15	4.44	3			4.46	8		
PV 19, γ mod	4.33	12			4.39		4.30	7							4.34	6
PR 83 (+gypsum?)	4.12	17			4.25/4.28		4.16	29	4.11	19						
PV 19, γ mod					4.08										4.07	2
PR 83/PV 19, β mod	4.00	86	3.91	3	3.91/4.00 (s)		4.04	10	4.03	17	4.04	20				
calcite	3.85	9	3.85	12	3.84 (s)	28										
PR 83/PV 19, γ mod	3.72/3.76	39	3.71	8			3.78	38	3.72	10	3.77	7			3.74	6
					3.62 (s)											
missing?							3.57	30							3.55	4
PV 19, α mod	3.45	68	3.42	23									3.45	42		
PV 19, γ mod	3.38	68	3.37	41											3.37	25
PV 19, γ mod	3.32	51	3.34	16	3.35										3.34	16
PV 19, β mod									3.28	97	3.28	100				

[a] ICDD reference data for the β-, α-, and γ-quinacridones is shown for comparison. *d* = *d*-spacing; *I* = phase intensity; sh = shoulder; b = broad; s = sharp; mod = crystal modification.

observed in modern paintings and also the overall thickness of the commercial paint film samples that were spread onto glass slides and examined under similar conditions, as described above.

The μXRD patterns obtained from the model paint system containing PY 1 in its top layer at various angles of incidence with respect to the specimen surface (Figure 1C), where $\omega = 0.25-2°$ and $\varphi = 360°$ rotation, illustrate that, in all cases, the X-ray penetration in the model samples is near or exceeds about 100 μm, i.e., through to the calcite layer. Results also demonstrate that the angle of incidence changes the X-ray cross section in the paint layers. As shown by the relative intensity of the calcite 100% line, at $\omega = 0.25°$, i.e., at a grazing angle of incidence, the highest proportion of the bottom calcite layer is detected. This is most likely due to the incident beam hitting the cut side of the sample, which was not completely flat, thus penetrating the entire cross section. On the other hand, when $\omega = 1-2°$, significantly less calcite is detected, showing that the calcite layer is attenuated by the top two layers at a glancing angle. At $\omega = 1°$, the depth of penetration through the three layers is the least under the experimental conditions used.

Many of the commercial paint films examined here contain fillers and pigments with relatively heavy metals, including zinc and barium. In particular, the presence of barite ($BaSO_4$) is expected to limit the penetration of the X-ray beam, which is estimated to be about 10–20 μm in the samples examined in this study. While the presence of barite, which is a very good scatterer, tends to swamp out minor phases, peaks related to many crystalline SOPs tend to correspond to large *d*-spacing and thus are not subject to major interference from peaks arising from either barite or other common inorganic pigments and fillers. These considerations have bearing on the interpretation of the additive phase patterns from paint samples removed for works of art.

Commercial Paints. One representative example of commercial paints bound in each of three major types of media, i.e., acrylic, alkyd, and oil, respectively, is discussed below. Additional data pertaining to seven other paint samples examined as part of this study may be found in the Supporting Information, Table S-1 and Figures S-21–S-27.

Acrylic Paints. For modern synthetic organic pigments, Raman bands due to the aromatic C–H stretches are expected in the range of 3100–3000 cm^{-1}; however, the analysis of the bands in the functionality that range below 1800 cm^{-1} is sufficient to identify and differentiate these pigments.[10–12] The Raman spectrum recorded for the acrylic paint Gruden (Professional) Yellow Medium Azo, designated as sample 3AC, shows bands consistent with the presence of a mixture of PY 83 and PY 74, diarylide and monoazo yellow pigments, respectively (Figures 2A and S-28 in the Supporting Information). Raman bands characteristic of TiO_2 in its rutile form at ca. 609 and 447 cm^{-1} [28] appear as very weak shoulders of the PY 74 bands at ca. 601 and 441 cm^{-1}. Rutile is declared as a component of the paint by the manufacturer.

Figure 2B compares the μXRD patterns obtained from the paint sample 3AC with the patterns recorded for the PY 83 and PY 74 powder samples and the ICDD references (vertical bars and Tables S-1, S-5, and S-6 in the Supporting Information). Results allow straightforward identification of PY 83 and PY 74 as separate, additive phases, along with the rutile form of TiO_2. Results thus demonstrate the potential of XRD to provide good qualitative identification for the SOPs and extenders in situ in the acrylic paint film, as well as confirmation of the Raman results. XRD results also appear typical in terms of limited line shifting and intensity changes compared to both the powder sample and the ICDD references, especially for the PY 83 phase, for which two reference patterns for the pigments were found in the ICDD database. In addition, several unidentified peaks exist near $d = 9.60$, 6.34, 5.31 and, most notably, 3.50 Å. The latter peak appears to be resolved from a shoulder on the 82% line in the pattern of the powder pigment PY 83. These unidentified, shifted, and/or narrower peaks suggest the presence of impurities and crystal quality differences, especially of PY 83, which is known to have one crystal form and an inability to form solid solutions.[30] The differences noted between reference and experimental patterns nevertheless do not inhibit the generic identification of the pigment.

Consistent with results obtained for sample 3AC, the remaining commercial paint samples bound in acrylic analyzed in the present study produced generally good quality XRD data that was complementary to the molecular information contained in Raman spectra and allowed the firm identification of the SOPs and extenders present (Table S-1 and Figures S-21–S-23 in the Supporting Information).

Alkyd Paint. The alkyd bound paint sample 1AD, Ferrario red Lacca Garanza Rosa, gave a weak Raman spectrum superimposed on a strong fluorescent background (shown in Figure 3A, top spectrum, after baseline correction). This spectrum is compared to that recorded for a sample of a violet quinacridone pigment PV 19 (Ciba) in Figure 3A (bottom spectrum), a sample which was also examined by μXRD (discussed above) and identified predominantly as the β modification of PV 19. Bands in the spectrum of 1AD at ca. 1317 and 1244 cm^{-1} are shifted to ca. 1310 and 1239 cm^{-1}, respectively, in the spectrum of the reference powder sample. Band positions in the Raman spectrum of 1AD appear to be consistent with those published for the γ modification of PV 19.[31] However, the Raman spectrum of the γ form has been reported to be similar to that of the β modification, while the infrared spectra of the two forms can be distinguished, according to some authors.[24,31] To our knowledge, no Raman spectra of the pure α or ε modifications of PV 19 have been reported, nor has crystallinity in this pigment been normally inferred from features in the Raman spectra.

Raman peaks characteristic of calcite (ca. 1087 cm^{-1}), gypsum (ca. 1008 cm^{-1}),[27] and PR 83 (ca. 1482, 1329, 1296, 1192, and 485 cm^{-1} [13]) are present in the spectrum recorded for 1AD. The PR 83 band at ca. 1329 cm^{-1} overlaps with a peak of the PV 19 reference at ca. 1332 cm^{-1}.

The μXRD diffraction pattern of sample 1AD is shown in Figure 3B along with the patterns obtained from the PV 19 powder sample

(29) Burgio, L.; Clark, R. J. H. *Spectrochim. Acta, Part A* **2001**, *57*, 1491.
(30) Barrow, M. J.; Christie, R. M.; Badcock, T. D. *Dyes Pigm.* **2002**, *57*, 99–106.
(31) Binant, C.; Guineau, B.; Lautie, A. *Spectrochim. Acta, Part A* **1989**, *45* (12), 1279–1287.

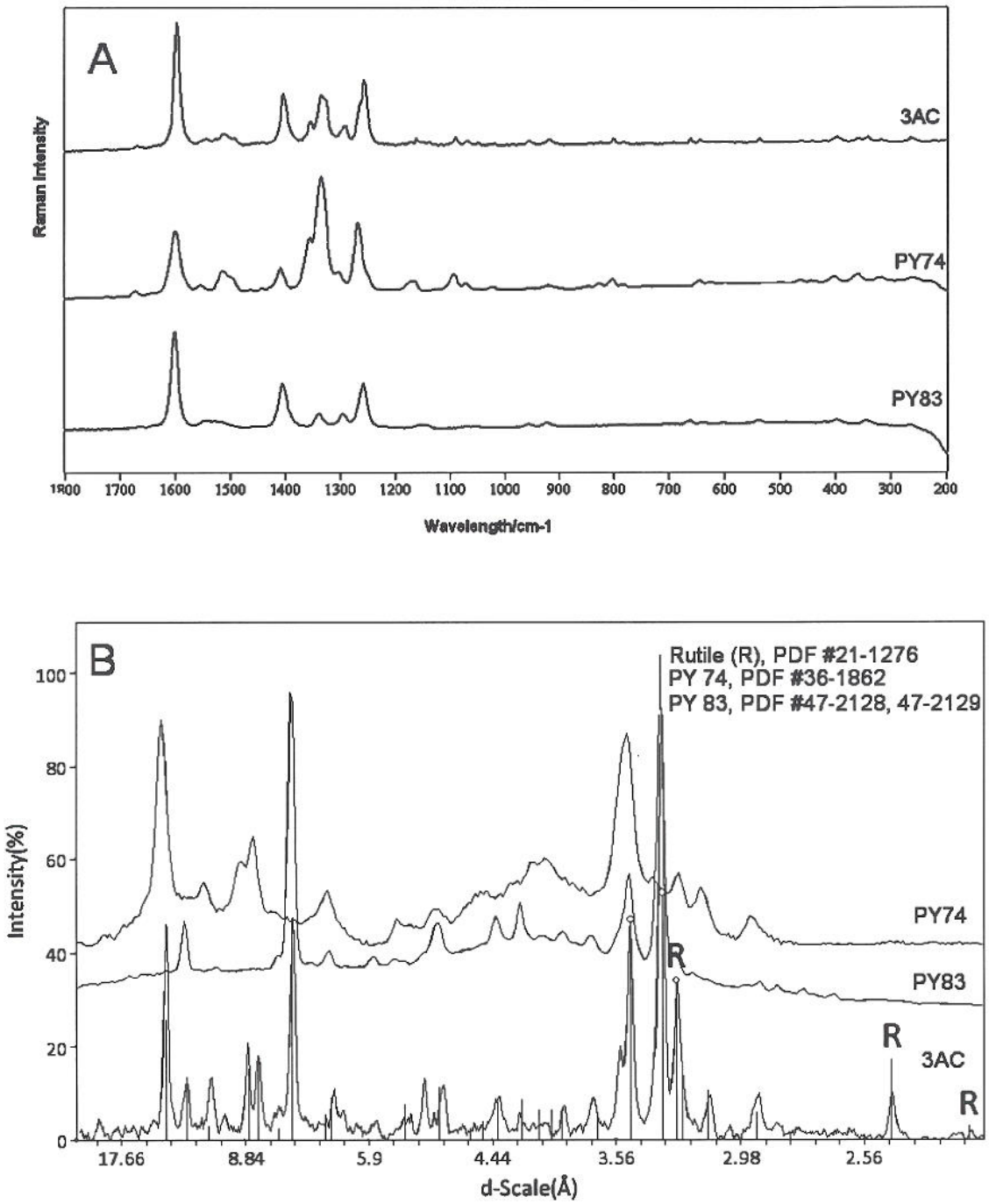

Figure 2. (A) Raman spectra of the acrylic bound sample 3AC (Gruden (Professional) Yellow Medium Azo, top spectrum), PY 74 (Ciba, middle spectrum), and PY 83 (SunChemicals, bottom spectrum) reference samples; $\lambda_0 = 785$ nm. (B) Details of μXRD patterns (Cu Kα radiation) obtained from pure pigments PY 74 (SunChemicals, top) and PY 83 (SunChemicals, middle) and paint sample 3AC, after background subtraction (bottom), shown with ICDD pattern matches in vertical bars (rutile marked with "R").

(Ciba, also shown in Figure 1B) and the pure pigment powder PR 83. Data obtained by μXRD with both Cr and Cu Kα radiation, as well as with open architecture XRD, is presented along with reference data in Table 2 (and Tables S-1, S-10, and S-15 in the Supporting Information). As shown in Table 2, only small differences in the experimental patterns acquired with Cr Kα or Cu Kα radiation are observed, although the former appears slightly improved in terms of peak resolution but slightly worse in terms of peak to background ratio (as in other experimental patterns). Agreement between results for peak positions for all three techniques is generally quite good, within experimental error; differences in relative intensities are more significant, however, most likely due to sample texture, which is unexpected in a well-dispersed paint film. Several additional peaks detected by open architecture XRD may be related to an unidentified contaminant in the sample. Results are somewhat inconsistent for the presence of gypsum, which is only tentatively identified and appears to be highly oriented.

In addition to reference pattern matches for calcite and possibly gypsum, the paint sample diffraction patterns show a series of

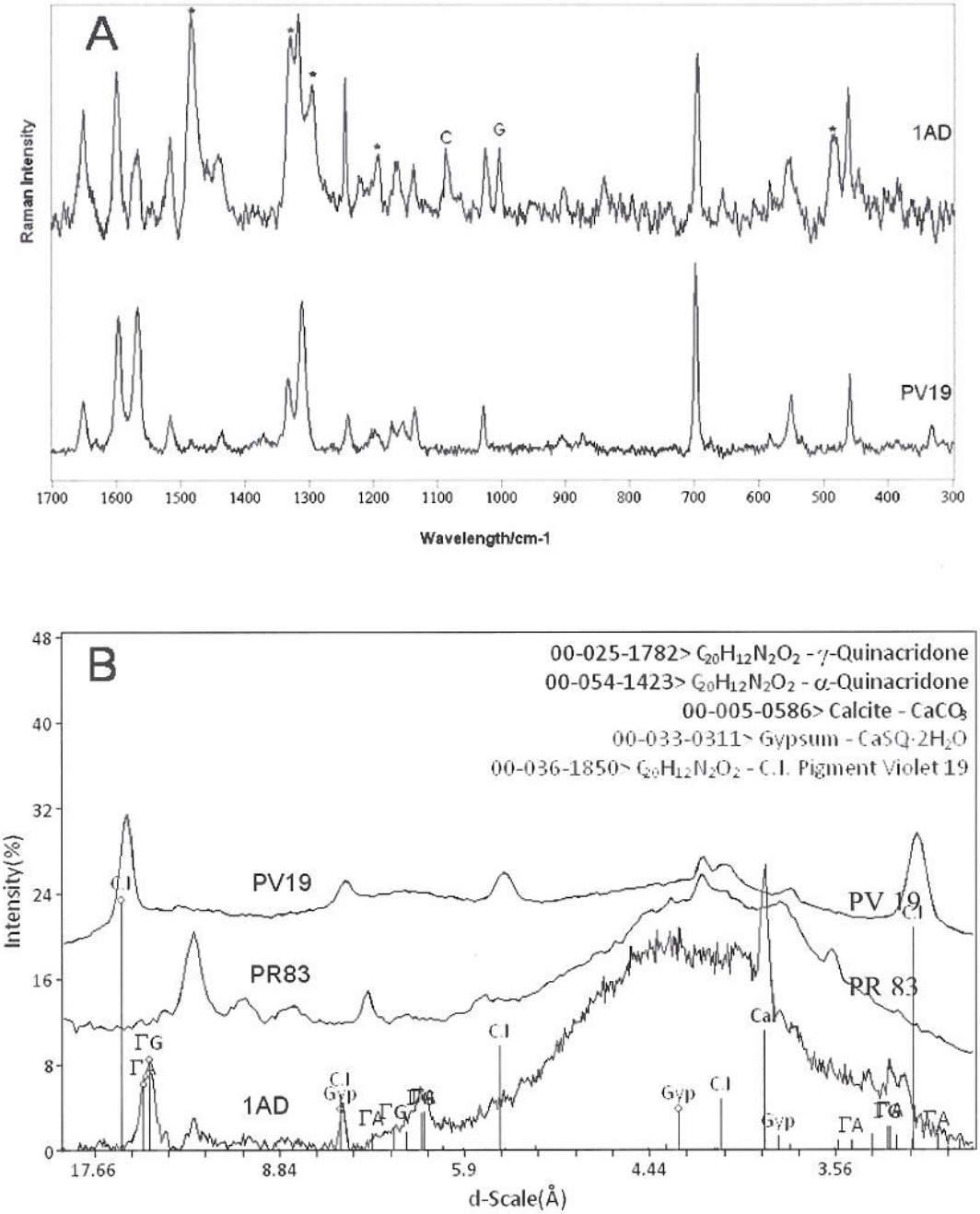

Figure 3. (A) Raman spectra of the alkyd bound sample 1AD (Ferrario (Alkyd) Lacca Garanza Rosa, top) and of a PV 19 reference sample (Ciba, bottom). Peaks due to PR 83 are indicated by asterisks, while C and G marked peaks are due to calcite and gypsum at ca. 1087 and 1008 cm^{-1}, respectively; $\lambda_0 = 785$ nm. (B) Details of μXRD patterns (Cu Kα radiation) obtained from pure pigments PV 19 (Ciba, above) and PR 83 (Schmincke, middle), with a pattern from paint sample 1AD (bottom), shown with ICDD pattern matches in vertical bars (PV 19 marked with "CI"; calcite marked with "Cal"; α-quinacridone marked with "ΓA"; γ-quinacridone marked with "ΓG"; gypsum peaks marked with "Gyp").

relatively broad peaks at large *d*-spacings that do not produce ICDD search matches for either PR 83 or the β-quinacridone form of PV 19. As previously mentioned, PR 83 was not found in the PDF 2007 ICDD database, which includes an organic pigment database. However, comparison to the XRD pattern of the pure pigment powder sample of PR 83 (Figure 3B, Table 2) confirms that this SOP can in fact be identified in the paint sample from its 100% line, as well as from at least two smaller, rather broad peaks that are most readily distinguished in the Cr Kα pattern. The poor definition of these peaks suggests rather small particle size (and/or particle strain) of the SOP in the paint vehicle.

The remaining peaks in the experimental patterns for 1AD (Figure 3B, Table 2) best match a combination of α and γ crystal modifications of the PV 19 pigment, although δ and ε forms found in the ICDD database (PDF #43-1515 and 48-2094) are also consistent with the patterns; the latter crystal forms are not widely accepted and are, therefore, not shown.[27,28] In addition, the pattern produced by open architecture XRD exhibits a peak shoulder that

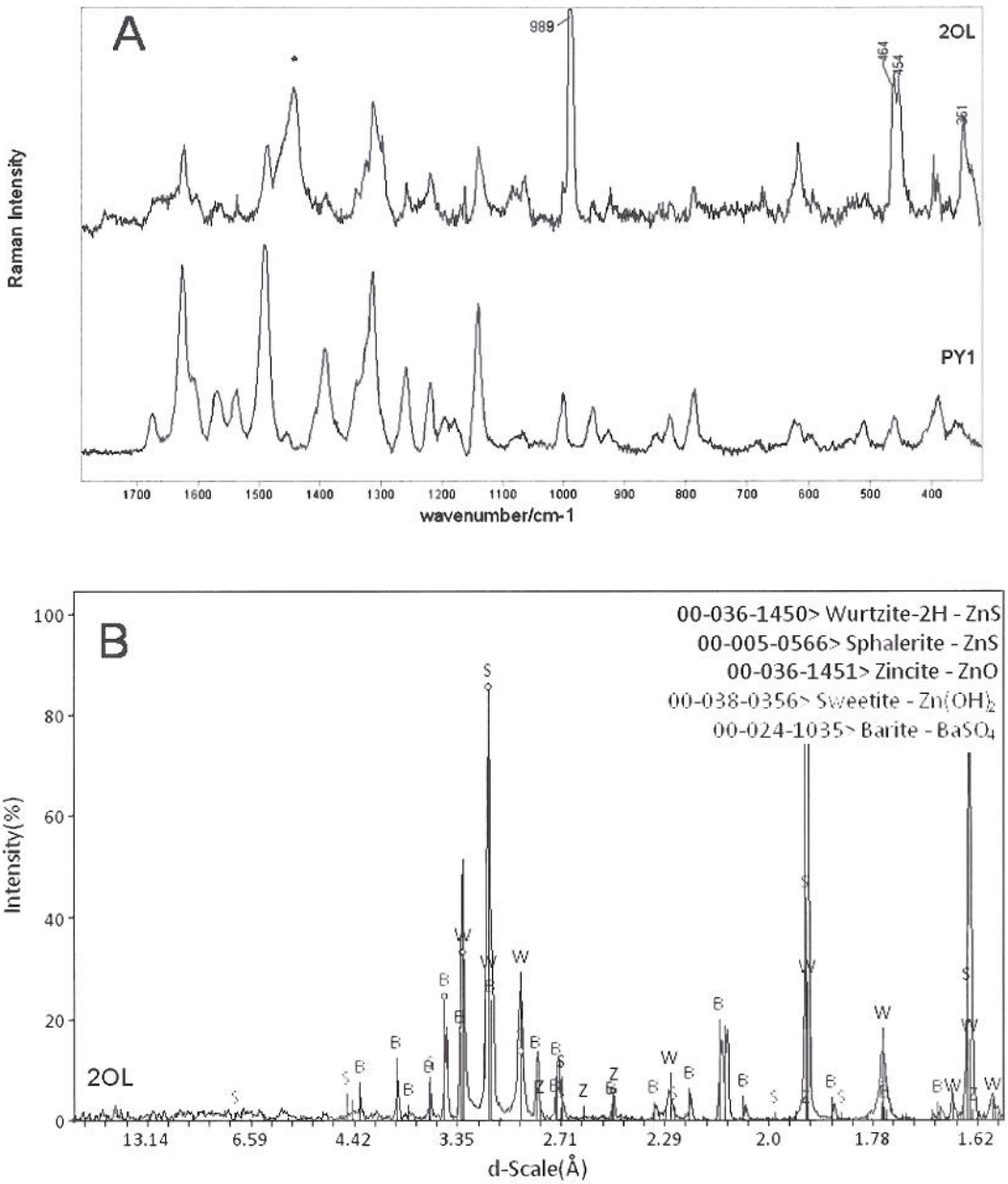

Figure 4. (A) Raman spectra of the oil bound sample 2OL (Lukas (Studio) Brillantgelb hell, top) and of a PY 1 reference sample (SunChemicals, bottom). Main bands are due to the extenders $BaSO_4$ (ca. 989 cm^{-1}, shown out of range, 464 and 454 cm^{-1}) and ZnS (ca. 351 cm^{-1}) indicated. The band at ca. 1440 cm^{-1}, marked by an asterisk, may arise from CH_2 deformations of the oil binder; λ_0 = 785 nm. (B) μXRD pattern detail (Cr Kα radiation) of paint sample 2OL, after background subtraction, with ICDD pattern matches shown in vertical bars (barite peaks marked with "B"; zincite peaks marked with "Z"; sweetite peaks marked with "S"; wurtzite peaks marked with "W"; sphalerite peaks marked with "S").

suggests the presence of the β-quinacridone as a minor phase. The identification of several polymorphs of the linear unsubstituted quinacridone in this case is significant, since the α form is known to be unstable[5,28] and, to our knowledge, there is no published data pertaining to crystal forms of the pigment found in works of art. Discussion of how crystallinity may affect aging properties of the paints is also lacking in the literature. This example, therefore, highlights the ability of XRD to provide important information that is complementary to Raman spectroscopy. XRD allows confirmation of tentative phases and clarifications about crystal quality and the presence of crystal modifications that may significantly impact physical properties of artists' paint films.

Oil Paints. The Raman spectrum recorded for the Lukas (Studio) Brillantgelb hell paint film, designated sample 2OL, presented a strong fluorescent background and is shown in Figure 4A (top) after baseline correction. Comparison of this spectrum with that recorded for a PY 1 powder reference sample (Figure 4A, bottom) indicates that this SOP is the main colorant in the sample. In the Raman spectrum of 2OL, the very strong band at ca. 989 cm^{-1} and the medium intensity features at ca. 464 and 454 cm^{-1} indicate the presence of the extender $BaSO_4$;[29] the peak at 464 cm^{-1} overlaps with a weak band of PY 1 at ca. 460 cm^{-1}.[10] The band expected at ca. 438 cm^{-1} for the extender zinc white (ZnO),[29] listed by the manufacturer, is not visible

in this spectrum. ZnS is present, as indicated by the peak at ca. 351 cm^{-1}, although no features that distinguish the ZnS cubic (sphalerite) and hexagonal (wurzite) modifications can be observed.[32] The presence of $BaSO_4$ and ZnS suggests that these compounds were added in the form of lithopone.[33] The strong band at ca. 1440 cm^{-1} in the spectrum of sample 2OL does not match Raman characteristic bands of SOPs in published databases[10,12,13] and may be assigned to CH_2 deformations of the oil binder reported at ca. 1438−1439 cm^{-1}.[34]

A detail of the μXRD pattern of sample 2OL is shown in Figure 4B (Table S-1 in the Supporting Information). This pattern exhibits peaks solely from inorganic pigments, indicating a combination of the zinc sulfides wurzite and sphalerite, plus barite (slightly shifted), confirming the identification of lithopone. In addition to ZnO (zincite), which is confirmed by XRD, zinc hydroxide (sweetite) is indicated. The latter mineral could be an alteration product of zincite; this is an interesting and unexpected result.

Surprisingly, the SOPs were not detected by μXRD either in this sample or in any of the four other oil paint samples examined (patterns not shown; see Table S-1 in the Supporting Information). The reasons underlying these results are unclear and will be the subject of future study. Possible explanations to be investigated include disruption of order in the SOP from interaction with the drying oil medium (primarily polyunsaturated glycerides) and/or dispersants.[35] It is known that some pigments tend to induce crystallization (nucleation) of semicrystalline polymers, so the reverse also seems possible. Although the same SOPs are normally used by paint manufacturers "as received" in different media, i.e., pigments with the same crystallite size are mixed into the oil, acrylic, or alkyd,[36] future work will also investigate whether different dispersion or milling effects may arise in paint mixing processes that affect the pigment crystallinity. As noted by Agashe,[37] primary particles of pigments may increase in size when mixed into a polymer. As noted by Hao and Iqbal[15] and Whitaker,[22] immediately after grinding or precipitation, some SOPs tend to show low crystallinity with many defects; this would adversely affect pigment performance.

In summary, it appears that Raman analysis is a superior method for the identification of SOPs in oil media, at least for the samples examined in this study (Figures S-24−S-29 in the Supporting Information). However, XRD in this case remains an important complement for the detailed and definitive identification of the inorganic pigment components in the paint formulation. As in the case of the commercial pigment powder samples, the patterns acquired for the acrylic, alkyd, and oil paints stand themselves as new XRD references of specific commercial artists' materials for their future identification in works of art.

(32) Brafman, O.; Mitra, S. S. *Phys. Rev.* **1968**, *171* (3), 931–934.
(33) Eastaugh, N.; Walsh, V.; Chaplin, T.; Siddall, R. *Pigment Compendium. A Dictionary of Historical Pigments*; Elsevier and Butterworth-Heinemann: Amsterdam, The Netherlands and Oxford, 2004.
(34) Vandenabeele, P.; Wehling, B.; Moens, L.; Edwards, H.; De Reu, M.; Van Hooydonk, G. *Anal. Chim. Acta* **2000**, *407*, 261.
(35) Personal communication from Dr. Jeffrey Post, Geologist and Curator-in-Charge, Mineral Collection, Smithsonian Museum of Natural History, January 2009.
(36) Personal communication from Jim Hayes, Technical Director, Golden Artist Colors, Inc., January 2009.
(37) Agashe, N.; Beaucage, G. Advanced Photon Source Activity Report 2001, ANL-02/06 Dec. 2002; pp 3, http://www.aps.anl.gov/apsar2001/AGASHEN1.pdf.

CONCLUSION

While Raman spectroscopy has recently been demonstrated to offer a significant advance in the study and identification of SOPs, particularly as a noninvasive technique, XRD is demonstrated here to be an effective and complementary tool for highly specific identification of synthetic organic pigments and their polymorphs, as well as fillers and inorganic pigments, in acrylic and alkyd bound artists' paints. In many cases, inorganic components from the fillers do not substantially interfere with the identification of the SOPs in the paint samples by XRD. Fillers (and extenders) such as $BaSO_4$ and, to a lesser degree, $CaCO_3$ may also limit the depth of penetration of the X-rays into the paint film. The identification of synthetic organic pigments by XRD in oil bound paints, however, appears problematic for reasons that are not yet determined. Raman spectroscopy has the additional advantage that it can be used both in microsamples and in situ in works of art in a noninvasive manner, although in situ XRD analysis, such as in an open architecture unit, is also feasible for small works of art. Both techniques appear to work satisfactorily as a tool for this type of investigation. As demonstrated, combined Raman spectroscopy and XRD may allow pigment and filler identification that would be tentative or difficult with either technique alone. As a complement to Raman, XRD analysis of SOPs also reveals information concerning crystal form and quality that cannot otherwise be readily obtained. These structural and formulatory details may have significant impact on pigment physical properties and durability. XRD thus has the potential to play an important and as yet unrealized role in the study of synthetic pigment in modern and contemporary works of art.

ACKNOWLEDGMENT

The authors are indebted to Lori Fields, Application Scientist at Rigaku America; Lee Daniels, Director of Small-Molecule Crystallography at Rigaku America; Tony Frantz, Research Scientist at the Metropolitan Museum of Art (MMA); Jeffrey E. Post, Geologist and Curator-in-Charge of the Mineral Collection at the Smithsonian National Museum of Natural History; Jim Hayes, Technical Director at Golden Artist Colors; and Giacomo Chiari, Chief Scientist, The Getty Conservation Institute, for generously sharing their expertise in helpful discussions, and to Marion Mecklenburg, Research Scientist at the Museum Conservation Institute (MCI), Smithsonian Institution, for aid and advice on the creation of model paint films. The authors are also grateful to Bob Koestler, Director at MCI; Jeff Speakman, Head of Technical Studies at MCI; Marco Leona, David H. Koch Scientist in Charge, Department of Scientific Research, MMA; Dianne van der Reyden, Director of Preservation Directorate; and Eric Hansen, Chief of Preservation Research and Testing, Library of Congress for their support.

SUPPORTING INFORMATION AVAILABLE

Additional information as noted in text. This material is available free of charge via the Internet at http://pubs.acs.org.

Received for review March 6, 2009. Accepted June 8, 2009.

AC9004953